Interacting Quasi-Two-Dimensional Sheets of Interlinked Carbon Nanotubes: A High-Pressure Phase of Carbon

Sumit Saxena* and Trevor A. Tyson*

Department of Physics, New Jersey Institute of Technology, Newark, New Jersey

ARTICLE

ABSTRACT A novel quasi-two-dimensional phase of carbon and the formation of a metastable hexagonal phase of single-walled carbon nanotubes (SWCNTs) have been investigated using density functional theory (DFT) by subjecting the SWCNT bundles to hydrostatic pressure. The chirality of the nanotubes determines the breaking of symmetry of the nanotubes under compression. Interestingly SWCNTs are found to undergo a mixture of sp^2 and sp^3 hybridization and are found to form novel interacting quasi-two-dimensional sheets of interlinked SWCNTs under hydrostatic pressure. Symmetry breaking, leading to the formation of highly directional bonds at stressed edges, is found to play an important role in the interlinking of the nanotubes. $(3n + 3, 3n + 3)$ SWCNTs are found to acquire a hexagonal cross-section when subjected to hydrostatic pressures. The opening of a pseudogap is observed for small as well as large diameter armchair SWCNTs in nanotube bundles. Equilibrium separations calculated using the Leonard-Jones potentials indicate excellent agreement with the predictions of density functional calculations and experimental observations.

KEYWORDS: carbon nanotubes · density functional theory · hydrostatic pressure · van der Waals · electronic structure

Carbon is a unique element that is known to exist in several allotropic forms such as diamond, graphite, amorphous carbon, fullerenes,[1] lonsdaleite,[2] and nanotubes[3] formed normally and under extreme conditions of temperature and pressure. These allotropic forms show a variety of interesting properties. The availability of a broad range of electronic properties makes SWCNTs[4] versatile and exceptional nanostructures unparalleled by any other material for nanoelectronic devices applications.[5] SWCNTs show extraordinary strength along the axial direction with a commonly accepted axial Young's modulus value of ~1 TPa.[6,7] Radial and axial[8−11] deformations of SWCNTs has attracted much attention as it is possible to influence their structural and electronic properties. The deformation of large diameter SWCNTs under pressure to interacting elliptic-, racetrack-, and peanut-shaped cross sections have been reported both experimentally[12,13] and theoretically.[14,15] The structural changes of large diameter nanotubes have also been observed indirectly using Raman spectroscopy and directly using x-ray[16] and neutron[17] diffraction experiments. The application of pressure on single-walled carbon nanotubes has brought to light a number of interesting properties[18] such as metal−insulator transitions.[19] The study of SWCNTs under pressure has also gained momentum recently because of the search for novel forms of carbon other than diamond, graphite, and carbon nanotubes consisting of a mixture of sp^2 and sp^3 hybridized carbon. These novel forms of carbon are thought to consist of both sp^2 and sp^3 hybrid states of carbon. Earlier studies have shown that only small diameter zigzag SWCNT bundles form interlinked structures when subjected to high hydrostatic pressure.[20] However, the modification in their electronic properties is still unknown. Compressed nanotubes are expected to exhibit different $\sigma^*-\pi^*$ hybridization. It would therefore be interesting to explore the possibilities of formation of novel forms of carbon at high pressures.

In this article we report the formation of novel interacting quasi-two-dimensional sheets of interlinked carbon nanotubes using ground state DFT. We find that this phenomenon occurs in both zigzag and armchair SWCNTs for small and large diameter nanotubes at high pressures. We also find that nanotubes with chiral indices $(3n + 3, 3n + 3)$ forms a metastable hexagonal phase under pressure. The formation of hexagonal cross sections at low pressure and novel interlinked structures are insensitive to the form of exchange correlation or the form of the potentials used. The opening of a pseudoband gap for armchair nanotubes is observed in excellent agreement with earlier tight binding,[21] ab initio methods

*Address correspondence to susax78@rediffmail.com, tyson@adm.njit.edu.

Received for review March 26, 2010 and accepted April 28, 2010.

Published online May 6, 2010. 10.1021/nn100626z

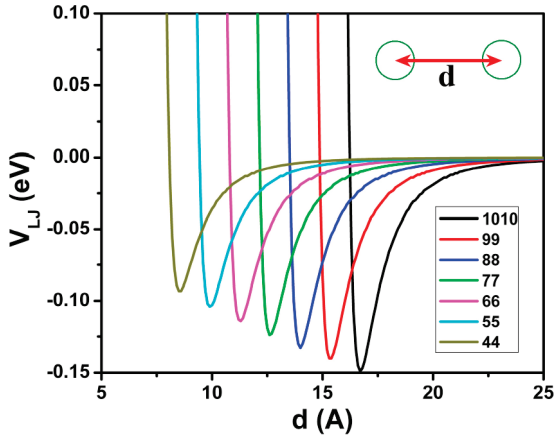

Figure 1. Interaction potential V_{LJ} (eV) per unit length as a function of the intertube separation *d* for different armchair nanotubes. The potential well becomes shallower for smaller diameter SWCNTs. The curve labels represent the chirality of the nanotube; that is, 1010 would mean armchair (10,10) SWCNT.

using local density approximation (LDA),[22,23] and experimental observations.[24] The effect of bundling on electronic band structure is also observed for zigzag nanotubes. Interacting SWCNTs were also studied using the Leonard-Jones (LJ) potential. It is observed that the findings of the DFT studies are in excellent agreement with the empirical model using the LJ potential containing the van der Waals (vdW) interactions, and these suggest that the DFT calculations work well for nanotube bundles under ambient and compressed conditions.

RESULTS AND DISCUSSION

Nanotubes packed in a triangular close-packed lattice with an intertube spacing of 3.3 Å which is typical of van der Waals interactions (vdW)[25] were considered. The calculated equilibrium intertube separation (*d*) at *ca.* 16.76 Å obtained using DFT is in close agreement to the experimentally[26] observed value of 16.95 (0.34) Å for the (10,10) nanotube. The value obtained using the LJ potential was found to be 16.70 Å. The interaction potential calculated as a function of distance *d* for different nanotubes using the LJ potential is shown in Figure 1. It is observed that the potential well becomes shallower with decreasing diameter of the nanotube. The equilibrium separation of ~3.15 Å between the tubes calculated using the LJ potential is in very good agreement with our DFT calculations. A comparative study of the DFT and LJ potential for graphitic systems has shown that both approaches agree very well at distances lower than the equilibrium separation.[27] The LJ potential describing the vdW interactions contains the London's (attractive) interactions that occur at large separations compared to the atomic radii. The delocalization energy has a shorter range than the exchange correlation energy. At large separations the exchange correlation is just the attractive term. At small separations the charge distribution overlaps producing a region of repulsion. The DFT underestimates these only at the large separation,[28] but does well for the repulsive part of the potential. Thus the DFT can be expected to correctly predict the response of SWCNTs under hydrostatic pressure.

We have studied the effect of increasing hydrostatic pressure using DFT on a large number of armchair and zigzag SWCNTs. We observe that the chirality of nanotubes determines the breaking of symmetry of the nanotubes under compression. This dictates the response of the SWCNTs to hydrostatic pressure. Our calculations show that $(3n + 3, 3n + 3)$ nanotubes deform under hydrostatic pressure such that the cross sections of these nanotubes gradually change from circular to hexagonal without any abrupt transformation as seen in Figure 2a for (6, 6) and (9, 9) SWCNTs. Interestingly the formation of hexagonal cross sections have been observed experimentally[29] for larger nanotubes of ~17 Å diameter during synthesis. The interaction between the walls of the nanotubes containing symmetrically placed atoms is expected to be the driving force prompting elastic deformation of nanotubes from a circular to hexagonal cross-section. The transition pressure from a circular to fully hexagonal cross-section is found to increase with decreasing tube radius as seen in Figure 2c−e due to increasing stiffness of the nanotubes. This hexagonal phase is a reversible phase and is expected to convert to peanut/racetrack-like cross sections at higher pressures. The formation of a hexagonal phase is also observed on changing the form of exchange correlation and the form of the potential as shown in the Supporting Information.

With further increase in pressure, formation of novel interlinked structures consisting of a mixture of sp^2 and sp^3 hybridized carbon atoms is observed for large (12, 12) SWCNTs as an abrupt change in the total energy and volume normalized with respect to total energy (E_0) and volume (V_0) under ambient conditions as shown in Figure 2a. The interlinked structure formed is shown in Figure 2b. The formation of an interlinked structure was verified by using USPP and PAW within the local density approximation. A comparative study has been shown in the Supporting Information.

Abrupt changes in energy and volume associated with changes in pressure are also observed for smaller (7, 0) and (5, 5) SWCNTs as seen in Figure 3a. Here also the formation of novel interacting quasi-two-dimensional structures accompanied by abrupt changes in energy−pressure and volume−pressure diagrams suggests a first order phase transition, clearly indicating formation of a new structural phase. At the onset of structural transitions the tubes form chemical bonds with each other. The atoms at highly stressed edges of the nanotubes link tetrahedrally by forming bonds with similarly stressed atoms in neighboring nanotubes. The stability of the novel interacting quasi two-dimensional structures was verified by releasing the

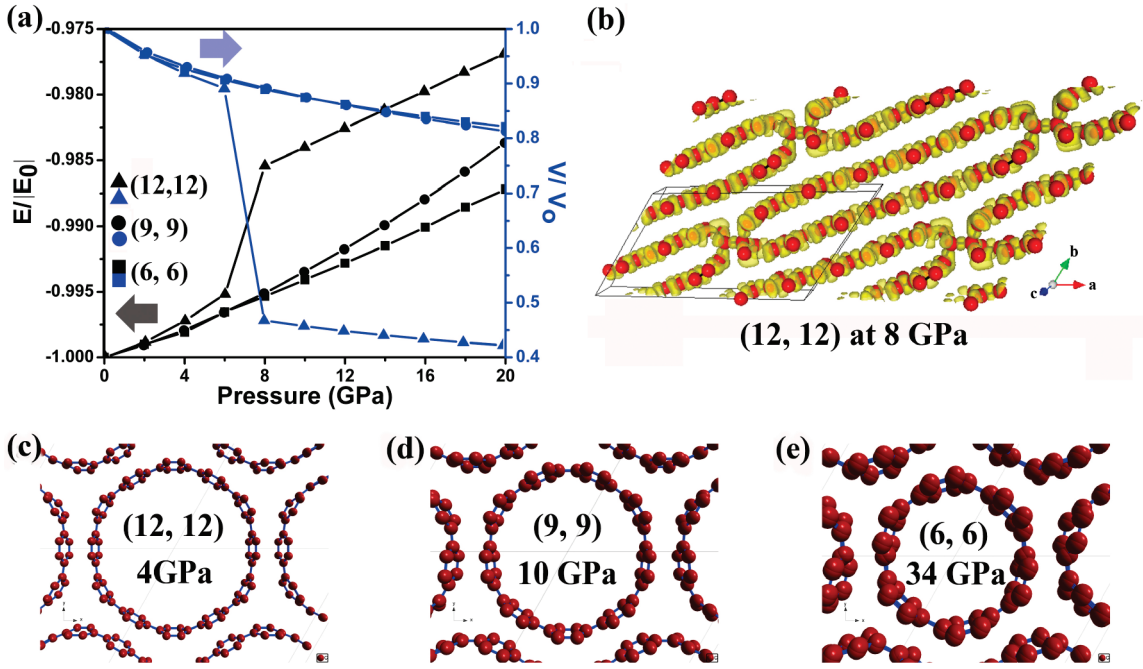

Figure 2. (a) Change in relative total energy and relative volume under hydrostatic pressure for (6, 6), (9, 9), and (12, 12) nanotubes; (b) interacting quasi-two-dimensional sheet of interlinked (12, 12) SWCNT at 8 GPa. Isosurface has been plotted at ELF value of 0.7. Hexagonal cross sections for (c) (12, 12), (d) (9, 9), and (e) (6, 6) SWCNTs under different hydrostatic pressures.

pressure. It is observed that when the pressure returned to ambient pressure, the interlinked structure is maintained. These observations are supported by recent experimental observations of a quenchable superhard carbon phase obtained by cold compression.[30] The peak in D band of Raman spectra in graphene indicates the presence of aromatic rings. The Raman spectra of an experimentally reported quenchable superhard carbon phase have two broad peaks centered at 1581 and 1355 cm^{-1} with the peak intensity of 1355 cm^{-1} (D band) which is much higher than that at 1581 cm^{-1} (G band). Studies on amorphous tetrahedral carbon films have shown that the ratio of the intensity of the peak in D band to that in the G band indicates the presence of sp^2/sp^3 bonding.[31] This suggests that the ratio of sp^3/sp^2 bonding is very small. The quasi-two-dimensional sheets of interlinked nanotubes obtained in our calculations are found to have sp^3 bonding only at stressed edges. These observations strongly support the formation of quasi-two-dimensional sheets of interlinked nanotubes as we have explicitly observed in these calculations. These calculations have shown that the separation between the flattened parts of the compressed nanotubes is ~3.3 Å as observed in graphite. However, XRD and TEM measurements have shown the lattice constant of this superhard carbon phase formed by compression at ~100 GPa is 2.1 Å. We expect that under extremely high hydrostatic pressures the repulsion is overcome and the separation between the walls of the nanotube decrease to smaller distances. No abrupt changes in energy were observed on compressing other small diameter nanotubes as seen in Figure 3b. These nanotubes get flattened gradually with increasing pressure. The tubes exhibit shearing resulting

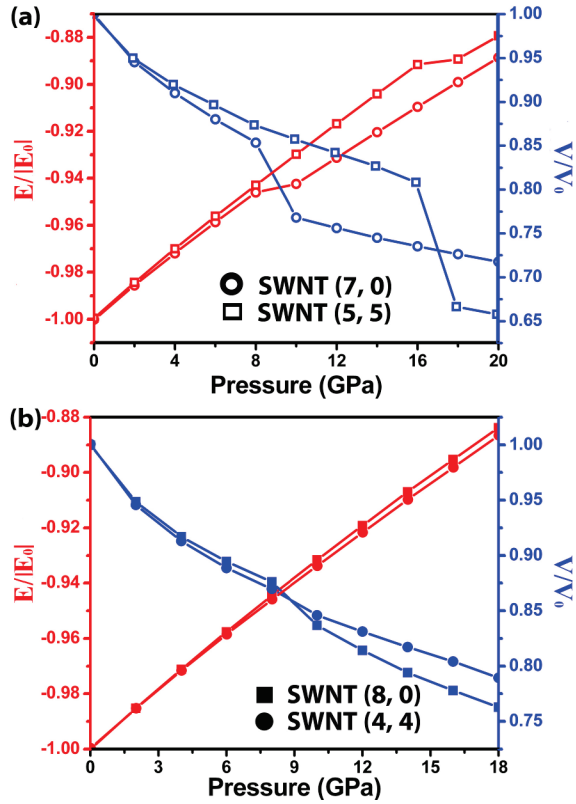

Figure 3. Change of relative total energy (*E*/*E*0) and relative volume (*V*/*V*0) under hydrostatic pressure of (a) (7, 0) zigzag and (5, 5) armchair SWCNT. Interlinked structures are formed at 10 and 18 GPa for (7, 0) and (5, 5) nanotubes respectively. (b) (8, 0) zigzag and (4, 4) armchair SWCNT.

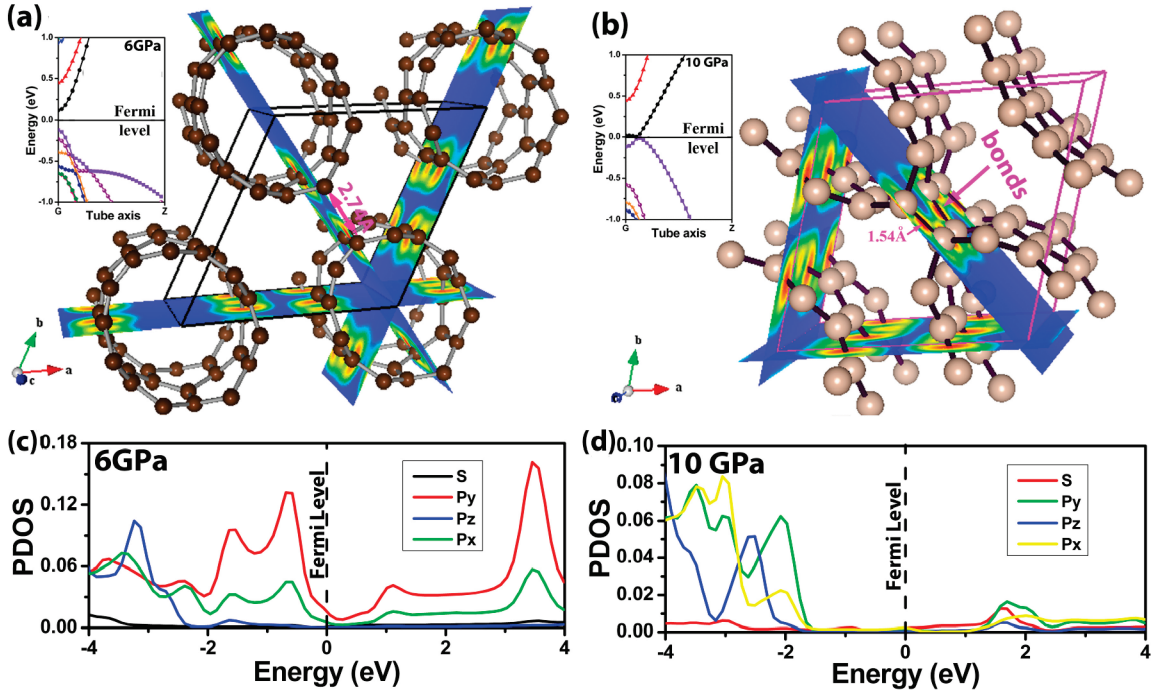

Figure 4. (a) Electron localization function (ELF) for (7, 0) nanotube at 6 GPa. The nanotubes are not bonded to each other; however, interaction cannot be ruled out at a separation of about 2.74 Å. The electronic band structure inset shows a small bandgap at the Fermi level. (b) ELF shows the interlinking of the tubes due to bond formation at 10 GPa along with the crossing of the conduction and the valence band at the Fermi level in the inset. The unit cells are marked with black (Figure a) and pink (Figure b) lines. PDOS for one of the highly stressed edge atom (c) at 6 GPa and (d) at 10 GPa.

in a reduction on both rotational and reflection symmetry with respect to the *z* axis.

Changes in electronic properties are expected to occur with changes in the atomic structure. The $\pi-\pi^*$ hybridization effect is understood to be a small contributing factor in changing the already existing band gap.[9] To understand the modification of the electronic properties we analyze the electronic band structure along with the partial density of states (PDOS). Abrupt phase transition is observed at a critical pressure P_c of about 10 GPa for the (7, 0) nanotube. We did a detailed investigation of the electronic properties at 6 and 10 GPa for this system. It is observed that at 6 GPa the distance between the adjacent atoms at the highly curved edges is about 2.76 Å; hence, any possibility of bond formation at this stage can be safely ruled out. The electron localization function[32] (ELF) provides a "chemically intuitive" way to analyze the electron localization and has values between 0 and 1. A high value implies that there is a high probability of finding two electrons of opposite spins in a given region of space along with a small probability of exchange with other electrons outside the region. The ELF was calculated for both armchair and zigzag carbon nanotubes using the formulation of Silvi and Savin.[33] The plot of electron localization function in Figure 4a shows that the tubes are not bonded to the neighbors under these conditions. Electronic band structure clearly shows in the inset of Figure 4a the presence of a small band gap at 6 GPa. These individual carbon nanotubes are semiconducting[34] under ambient conditions. As the pressure is increased, the symmetry of the nanotubes breaks such that highly directional ELF occurs at stressed edges. This results in strong bond formation between the atoms at the highly stressed edges with their neighbors in adjacent tubes as seen in the ELF plot in Figure 4b. This is accompanied by a crossing of the lowest conduction and valence band at the Fermi level indicating a metallic state of the interlined structure along the axis. It is interesting to note that the nanotubes interlink to form 2D layers of interlinked flattened tubes. Although no bond formation is observed between the sheets themselves, the sheets may interact with each other in a periodic manner because of reduced separation between them at these locations. We analyze the PDOS at the highly stressed sites at 6 GPa in Figure 4c and at 10 GPa in Figure 4d to understand the role of these atoms and the states associated with these atoms. We find that at 10 GPa the states move far away from the Fermi level. This is in accordance with the observation that the edge carbon atoms become stable sp^3-hybridized as found in diamond. The contribution to the DOS at the Fermi level is almost insignificant due to the pure p_x, p_y, and p_z orbitals at highly stressed edge atoms; hence, most of the contribu-

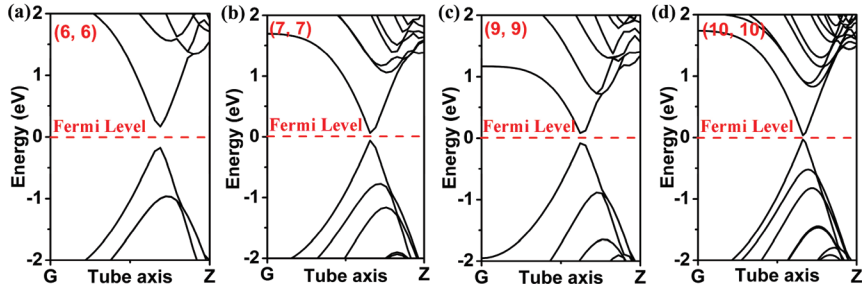

Figure 5. Electronic band structure for (a) (6, 6), (b) (7, 7), (c) (9, 9), and (d) (10, 10) armchair SWCNTs showing an opening-up of a pseudobandgap when bundled. The Fermi level has been adjusted to zero.

TABLE 1. Comparative study of the Pseudogap and Lattice Constant for (10, 10) SWCNT Obtained from Different Methods

method[a]	pseudogap (eV)	lattice constant (Å)
experiment[12,20]	~0.080[12]	16.95[20]
VASP LDA + USPP (Vanderbilt) + XC = CA	~0.186	16.85
VASP LDA + PAW + XC = CA	~0.179	16.42
VASP GGA + PAW + XC = PE	~0.066	16.66
LDA + PP (Troullier and Martin) + XC = CA[16]	~0.200	16.50
LDA + empirical PP[15]	~0.100	

[a]CA = Ceperley and Alder; PE = Perdew, Burke, and Ernzerhof; LDA = Local density approximation; USPP = Ultra soft pseudopotentials; PAW = Projector augmented wave; GGA = Generalized gradient approximation; PP = Pseudopotentials; XC = Exchange correlation.

tion to the DOS at the Fermi level due to pure p_x, p_y, and p_z orbitals is expected from other atoms at flattened surfaces.

The (5, 5) armchair nanotube is expected to be metallic under ambient conditions due to the crossing of bonding π and antibonding π^* bands at the Fermi level. An isolated (n, n) nanotube has n mirror planes containing the tube axis and it is the symmetry of the nanotube that gives the desired metallic character to this isolated nanotube. When bundled, a small perturbation adds to the Hamiltonian due to the influence of the neighboring tubes at the k points where the bands cross. This is also accompanied by the breaking of symmetry. This opens a very small pseudogap at the Fermi level as seen in Figure 5a−d. The density of states is suppressed and not exactly zero at the Fermi level; hence, the term pseudogap is commonly used. Our calculations show that the opening of the band gap is observed in both small (4, 4), (5, 5), (6, 6), (7, 7) and larger (9, 9), (10, 10), and (12, 12) diameter nanotubes. These observations are in accordance with experimental[12] observations of the opening up of a pseudogap in armchair nanotubes. A comparative study of the opening of the pseudoband gap obtained for different methods for the (10, 10) armchair SWCNT is shown in Table 1. The comparative study shows that the pseudobandgap is more accurately given by GGA while the lattice parameters predicted by LDA are closest to the experimentally obtained values. Symmetry is intrinsic to the electronic band structures; hence, one may expect change in the electronic structure at the Fermi level when symmetry is broken. We observe that when (5, 5) SWCNT is compressed the symmetry of the nanotube is lost, and the band gap widens to about 0.26 eV as shown in the inset of Figure 6a, indicating semiconducting behavior at about 16 GPa. At this stage the neighboring tubes with a separation of about 2.3 Å are not linked to each other as seen in the ELF plot in Figure 6a; however, increased interaction among the nanotubes can be seen. As the pressure is increased the tubes in the neighboring atoms link with each other forming highly interacting sheets as also observed in the zigzag (7, 0) nanotube. However, in this case the polygon enclosing the tetrahedral carbon atoms are

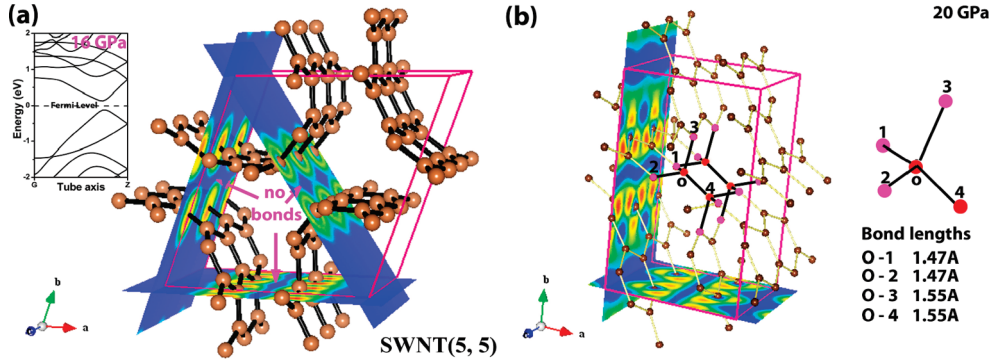

Figure 6. (a) Electron localization function (ELF) for the (5, 5) nanotube at 16 GPa. The nanotubes are not bonded to each other; however, interaction cannot be ruled out at a separation of about 2.74 Å. The electronic band structure inset shows a small bandgap at the Fermi level. (b) ELF shows the interlinking of the tubes due to bond formation at 20 GPa. The unit cells are marked with pink lines. Bonds labeled O-1 implies bond length from atom O to atom 1.

slightly distorted, as seen in Figure 6b. At this stage this sheet composed of interlinked (5, 5) nanotubes is found to show metallic properties with bands crossing the Fermi level. The interlinking of nanotubes is also found to occur for larger nanotubes as discussed earlier. The breaking of symmetry depends on the chiral indices of the nanotubes which determines the formation of directional bonds and hence the interlinking of nanotubes under compression. We observe that the nanotubes form interlinks with the neighboring tubes when highly directional dangling bonds are formed at the stressed edges of the cross sections. The availability of highly directional dangling bonds in close vicinity enables bond formation thereby reducing the energy of the system causing abrupt changes in the energy−pressure diagrams.

CONCLUSION

We have investigated the formation of novel interacting quasi-two-dimensional sheets of interlinked nanotubes by subjecting carbon nanotube bundles to hydrostatic pressure using DFT techniques. This is marked by a decrease in energy and observed as an abrupt change in the relative total energy−pressure diagram. The high pressure interlinked structures are stable and remain so upon releasing the pressure. Formation of metastable hexagonal cross sections for $(3n+3, 3n+3)$ nanotubes is observed at low pressures. The formation of a hexagonal phase for $(3n+3, 3n+3)$ SWCNTs at low pressure and the novel interacting phase is observed irrespective of the form of the exchange correlation or the potential used. Equilibrium separations in bundled carbon nanotubes calculated using LJ potentials are very close to the DFT results showing the accuracy of the approach. Our calculations reveal that the electronic band structure of all carbon nanotubes is modified when bundled due to the interaction with neighboring nanotubes. This modification of the electronic band structure is observed as the opening of a pseudogap in armchair SWCNTs.

Interacting quasi-two-dimensional sheets of interlinked nanotubes are stabilized due to the formation of highly directional dangling bonds at the stressed edges under compression. Our findings of the formation of interacting quasi-two-dimensional sheets of interlinked nanotubes are supported by previously reported experimental results and will motivate further research toward study and application of this novel quasi-two-dimensional form of carbon.

THEORETICAL METHODOLOGY

First principles ground state DFT calculations using the plane wave Vienna *ab initio* Simulation Package (VASP)[35,36] were performed. Spin restricted calculations within the generalized gradient approximation (GGA) were done using projector augmented wave[37] (PAW) potentials with the exchange correlation of Perdew−Burke−Ernzerhof (PBE). Calculations within the LDA using PAW and Vanderbilts ultrasoft pseudopotentials (USPP) using exchange correlation of Ceperley and Alder[38] as parametrized by Perdew and Zunger[39] were also performed to verify the formation of interacting quasi-two-dimensional sheets of interlinked carbon nanotubes and compare the results with that obtained using GGA. A high kinetic energy cutoff of 400 eV for the plane waves was used. The geometry was relaxed using the conjugate gradient technique such that no forces on atoms exceed 0.001 eV/Å. Electronic properties were calculated by sampling the reciprocal space using 30 *k*-points along the tube axis after the structural optimization. Hydrostatic pressure was monotonically increased in steps of 2 GPa for GGA calculations using PAW potentials and LDA calculations using USPP, while pressure steps of 4 GPa were used for LDA calculations using PAW potentials. The approach is consistent with that used in previous work.[40] The vdW interactions within the LJ model for the SWCNT−SWCNT interaction was calculated using the relation

$$V = \sigma^2 \int \int \left(-\frac{A}{r^6} + \frac{B}{r^{12}}\right) dS_1\, dS_2$$

The value of Hamaker constants were taken to be $A = 15.2$ eV Å, $B = 24 \times 10^3$ eV Å. The surface density of the SWCNTs were assumed to be uniform with $\sigma = 0.3724$[41,42] which is derived from graphene. The separation between two charge elements is represented by r, while dS_1 and dS_2 represent the surface elements. The vdW potential is derived by replacing the SWCNT by a shell of charge of surface σ density and then computing the interactions between the pair of tubes. The details of the vdW calculations are provided in the Supporting Information.

Acknowledgment. We acknowledge the computing time available to us on NJIT University computing facility "HYDRA" and NSF DMR Grant DMR-0512196 for this purpose.

Supporting Information Available: Comparison of LDA with GGA results; details of the vdW calculations. This material is available free of charge *via* the Internet at http://pubs.acs.org.

REFERENCES AND NOTES

1. Kroto, H. W.; Heath, J. R.; O'Brien, S. C.; Curl, R. F.; Smalley, R. E. C60: Buckminsterfullerene. *Nature* **1985**, *318*, 162–163.
2. Frondel, C.; Marvin, U. B. Lonsdaleite, a Hexagonal Polymorph of Diamond. *Nature* **1967**, *214*, 587–589.
3. Iijima, S.; Ichihashi, T. Single-Shell Carbon Nanotubes of 1-nm Diameter. *Nature* **1993**, *363*, 603–605.
4. Dai, H. Carbon Nanotubes: Synthesis, Integration, and Properties. *Acc. Chem. Res.* **2002**, *35*, 1035–1044.
5. Hatton, R. A.; Miller, A. J.; Silva, S. R. P. Carbon Nanotubes: A Multi-Functional Material for Organic Optoelectronics. *J. Mater. Chem.* **2008**, *18*, 1183–1192.
6. Salvetat, J.-P.; Briggs, G. A. D.; Bonard, J.-M.; Bacsa, R. R.; Kulik, A. J.; Stöckli, T.; Burnham, N. A.; Forró, L. Elastic and Shear Moduli of Single-Walled Carbon Nanotube Ropes. *Phys. Rev. Lett.* **1999**, *82*, 944–947.
7. Sears, A.; Batra, R. C. Macroscopic Properties of Carbon Nanotubes from Molecular-Mechanics Simulations. *Phys. Rev. B* **2004**, *69*, 235406–235415.
8. Mehrez, H.; Svizhenko, A.; Anantram, M. P.; Elstner, M.; Frauenheim, T. Analysis of Band-Gap Formation in Squashed Armchair Carbon Nanotubes. *Phys. Rev. B* **2005**, *71*, 155421–155427.
9. Park, C.-J.; Kim, Y.-H.; Chang, K. J. Band-Gap Modification by Radial Deformation in Carbon Nanotubes. *Phys. Rev. B* **1999**, *60*, 10656–10659.
10. Mazzoni, M. S. C.; Chacham, H. Bandgap Closure of a Flattened Semiconductor Carbon Nanotube: A First-Principles Study. *Appl. Phys. Lett.* **2000**, *76*, 1561–1563.

11. Saxena, S.; Tyson, T. A. *Ab Initio* Density Functional Studies of the Restructuring of Graphene Nanoribbons to Form Tailored Single Walled Carbon Nanotubes. *Carbon* **2010**, *48*, 1153–1158.
12. Merlen, A.; Bendiab, N.; Toulemonde, P.; Aouizerat, A.; San Miguel, A.; Sauvajol, J. L.; Montagnac, G.; Cardon, H.; Petit, P. Resonant Raman Spectroscopy of Single-Wall Carbon Nanotubes Under Pressure. *Phys. Rev. B* **2005**, *72*, 035409−035415.
13. Proctor, J. E.; Halsall, M. P.; Ghandour, A.; Dunstan, D. J. Raman Spectroscopy of Single-Walled Carbon Nanotubes at High Pressure: Effect of Interactions Between the Nanotubes and Pressure Transmitting Media. *Phys. Status Solidi B* **2007**, *244*, 147–150.
14. Lu, J. Q.; Wu, J.; Duan, W.; Liu, F.; Zhu, B. F.; Gu, B. L. Metal-to-Semiconductor Transition in Squashed Armchair Carbon Nanotubes. *Phys. Rev. Lett.* **2003**, *90*, 156601–156604.
15. Tangney, P.; Capaz, R. B.; Spataru, C. D.; Cohen, M. L.; Louie, S. G. Structural Transformations of Carbon Nanotubes Under Hydrostatic Pressure. *Nano Lett.* **2005**, *5*, 2268–2273.
16. Sharma, S. M.; Karmakar, S.; Sikka, S. K.; Teredesai, P. V.; Sood, A. K.; Govindaraj, A.; Rao, C. N. R. Pressure-Induced Phase Transformation and Structural Resilience of Single-Wall Carbon Nanotube Bundles. *Phys. Rev. B* **2001**, *63*, 205417–205421.
17. Rols, S.; Goncharenko, I. N.; Almairac, R.; Sauvajol, J. L.; Mirebeau, I. Polygonization of Single-Wall Carbon Nanotube Bundles Under High Pressure. *Phys. Rev. B* **2001**, *64*, 153401–153404.
18. Li, C.; Chou, T.-W. Elastic Properties of Single-Walled Carbon Nanotubes in Transverse Directions. *Phys. Rev. B* **2004**, *69*, 073401−073403.
19. Lammert, P. E.; Zhang, P.; Crespi, V. H. Gapping by Squashing: Metal-Insulator and Insulator-Metal Transitions in Collapsed Carbon Nanotubes. *Phys. Rev. Lett.* **2000**, *84*, 2453–2456.
20. Yildirim, T.; Gülseren, O.; Kilic, C.; Ciraci, S. Pressure-Induced Interlinking of Carbon Nanotubes. *Phys. Rev. B* **2000**, *62*, 12648–12651.
21. Delaney, P.; Choi, H. J.; Ihm, J.; Louie, S. G.; Cohen, M. L. Broken Symmetry and Pseudogaps in Ropes of Carbon Nanotubes. *Nature* **1998**, *391*, 466–468.
22. Delaney, P.; Joon Choi, H.; Ihm, J.; Louie, S. G.; Cohen, M. L. Broken Symmetry and Pseudogaps in Ropes of Carbon Nanotubes. *Phys. Rev. B* **1999**, *60*, 7899–7904.
23. Kwon, Y.-K.; Saito, S.; Tománek, D. Effect of Intertube Coupling on the Electronic Structure of Carbon Nanotube Ropes. *Phys. Rev. B* **1998**, *58*, R13314–R13317.
24. Ouyang, M.; Huang, J.-L.; Cheung, C. L.; Lieber, C. M. Energy Gaps in "Metallic" Single-Walled Carbon Nanotubes. *Science* **2001**, *292*, 702–705.
25. Chesnokov, S. A.; Nalimova, V. A.; Rinzler, A. G.; Smalley, R. E.; Fischer, J. E. Mechanical Energy Storage in Carbon Nanotube Springs. *Phys. Rev. Lett.* **1999**, *82*, 343–346.
26. Thess, A.; Lee, R.; Nikolaev, P.; Dai, H.; Petit, P.; Robert, J.; Xu, C.; Lee, Y. H.; Kim, S. G.; Rinzler, A. G.; *et al*. Crystalline Ropes of Metallic Carbon Nanotubes. *Science* **1996**, *273*, 483–487.
27. Girifalco, L. A.; Hodak, M. van der Waals Binding Energies in Graphitic Structures. *Phys. Rev. B* **2002**, *65*, 125404–125408.
28. Kohn, W.; Meir, Y.; Makarov, D. E. van der Waals Energies in Density Functional Theory. *Phys. Rev. Lett.* **1998**, *80*, 4153–4156.
29. López, M. J.; Rubio, A.; Alonso, J. A.; Qin, L. C.; Iijima, S. Novel Polygonized Single-Wall Carbon Nanotube Bundles. *Phys. Rev. Lett.* **2001**, *86*, 3056–3059.
30. Wang, Z.; Zhao, Y.; Tait, K.; Liao, X.; Schiferl, D.; Zha, C.; Downs, R. T.; Qian, J.; Zhu, Y.; Shen, T. A Quenchable Superhard Carbon Phase Synthesized by Cold Compression of Carbon Nanotubes. *Proc. Natl. Acad. Sci. U. S. A.* **2004**, *101*, 13699–13702.
31. Chhowalla, M.; Ferrari, A. C.; Robertson, J.; Amaratunga, G. A. J. Evolution of sp^2 Bonding With Deposition Temperature in Tetrahedral Amorphous Carbon Studied by Raman Spectroscopy. *Appl. Phys. Lett.* **2000**, *76*, 1419–1421.
32. Becke, A. D.; Edgecombe, K. E. A Simple Measure of Electron Localization in Atomic and Molecular Systems. *J. Chem. Phys.* **1990**, *92*, 5397–5403.
33. Silvi, B.; Savin, A. Classification of Chemical Bonds Based on Topological Analysis of Electron Localization Functions. *Nature* **1994**, *371*, 683–686.
34. Bulusheva, L. G.; Okotrub, A. V.; Romanov, D. A.; Tomanek, D. Electronic Structure of (*n*,0) Zigzag Carbon Nanotubes: Cluster and Crystal Approach. *The J. Phys. Chem. A* **1998**, *102*, 975–981.
35. Kresse, G.; Furthmuller, J. Efficient Iterative Schemes for *ab Initio* Total-Energy Calculations Using a Plane-Wave Basis Set. *Phys. Rev. B* **1996**, *54*, 11169–11186.
36. Kresse, G.; Furthmuller, J. Efficiency of *ab-Initio* Total Energy Calculations for Metals and Semiconductors Using a Plane-Wave Basis Set. *Comp. Mater. Sc.* **1996**, *6*, 15–50.
37. Kresse, G.; Joubert, D. From Ultrasoft Pseudopotentials to the Projector Augmented-Wave Method. *Phys. Rev. B* **1999**, *59*, 1758–1775.
38. Ceperley, D. M.; Alder, B. J. Ground State of the Electron Gas by a Stochastic Method. *Phys. Rev. Lett.* **1980**, *45*, 566–569.
39. Perdew, J. P.; Zunger, A. Self-Interaction Correction to Density-Functional Approximations for Many-Electron Systems. *Phys. Rev. B* **1981**, *23*, 5048–5079.
40. Nikitin, A.; Zhang, Z.; Nilsson, A. Energetics of C−H Bonds Formed at Single-Walled Carbon Nanotubes. *Nano Lett.* **2009**, *9*, 1301–1306.
41. Popescu, A.; Woods, L. M.; Bondarev, I. V. Simple Model of van der Waals Interactions Between Two Radially Deformed Single-Wall Carbon Nanotubes. *Phys. Rev. B* **2008**, *77*, 115443–115452.
42. Sun, C.-H.; Yin, L.-C.; Li, F.; Lu, G.-Q.; Cheng, H.-M. van der Waals Interactions between Two Parallel Infinitely Long Single-Walled Nanotubes. *Chem. Phys. Lett.* **2005**, *403*, 343–346.